VOLUME 72, NUMBER 2

JOC Articles

JANUARY 19, 2007

Tetrahedral Boron Chemistry for the Preparation of Highly Efficient "Cascatelle" Devices

Christine Goze, Gilles Ulrich,* and Raymond Ziessel*

Laboratoire de Chimie Moléculaire, Centre National de la Recherche Scientifique (CNRS), École de Chimie, Polymères, Matériaux (ECPM), 25 rue Becquerel, 67087 Strasbourg Cedex 02, France

gulrich@chimie.u-strasbg.fr; ziessel@chimie.u-strasbg.fr

Received May 11, 2006

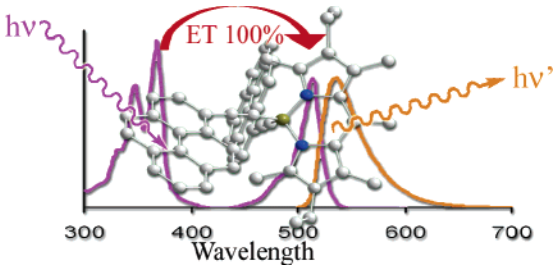

The replacement of the two fluorine atoms on the boron center of the well-known Bodipy fluorophore by functionalized acetylenic groups opens the way to a new family of highly luminescent, redox active, and stable fluorophores termed "*E*-Bodipy" species. The substitution is effective for ethynyl-lithium reagents incorporating tolyl, naphthyl, pyrenyl, fluorenyl, and terpyridinyl units. The protocol also tolerates the presence of various functional groups in the dipyrromethene meso position such as pyrene, phenylethynylpyrene, 4′-terpyridine, and iodophenyl. The last of these is particularly useful for a further coupling reaction enabling introduction of a flexible arm bearing a succinimidyl unit reactive toward primary amines. X-ray structure determinations of two *E*-Bodipy compounds confirm the introduction of the ethynyl units and show the boron atoms to have a distorted tetrahedral environment, with B−C(ethynyl) ∼1.59 Å and both boron atoms lying essentially in the mean planes of the dipyrromethene units. All the new compounds show intense electronic absorption bands (ϵ 60 000−70 000 M^{-1} cm^{-1}), high quantum yields (>80%), and slow rates of nonradiative decay. Absorption by the aromatic substituents results in a "cascatelle" process leading to emission exclusively through the boradiazaindacene entity and thus large virtual Stokes' shift (>10 000 cm^{-1}). The new compounds are also redox active, with the formation of both $Bodipy^{+\bullet}$ and $Bodipy^{-\bullet}$ occurring more readily than for *F*-Bodipy species. The molecules in their excited states are strong reducing agents.

Introduction

Boradiazaindacenes, commercially known as BODIPY dyes, are a family of very widely used fluorescent dyes. Their intense absorptions, high quantum yields, and tunable emission wavelengths make them good candidates for biological labeling applications.[1] However, the presence of BF bonds in the usual *F*-Bodipy dyes (Chart 1) results in some instability under irradiation and sensitivity to polar solvents, and *F*-Bodipys also share a disadvantage common to most organic fluorophores of small Stokes' shifts in their emission spectra. These small shifts necessitate narrow-band filters for labeling experiments and selective excitation sources for these red-emitting dyes. The

(1) Haughland R. P. *The Handbook A Guide to Fluorescent Probes and Labeling Technologies*, 10th ed.; Invitrogen: Carlsbad, CA, 2005.

10.1021/jo060984w CCC: $37.00
Published on Web 09/13/2006

CHART 1

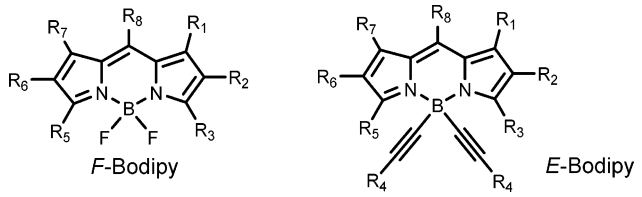

SCHEME 1 [a]

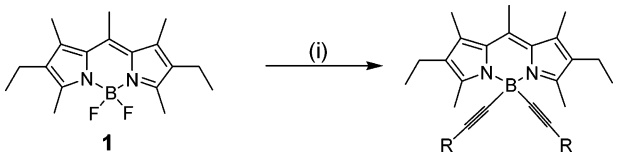

[a] Keys: (i) R−C≡C−Li, THF, rt, 5−30 min.

common approach to enhancement of Stokes' shifts is to unite two chromophores in one molecule, one taking the role of energy donor (high energy absorbing chromophore) and the other being the acceptor (lower energy emitting fluorophore). In such "cascatelle"[2] systems, a through space energy transfer process (i.e., Förster type)[3] is believed to occur, and this requires a significant overlap of the donor emission and acceptor absorption spectra, a requirement which makes the Stokes' shifts possible. In general, readily synthesized, highly luminescent dyes showing large virtual Stokes' shifts should find numerous applications in direct multicolor labeling experiments, obviating the need for highly sophisticated detection systems.[4] The development of fluorescent energy transfer devices on modified oligo-deoxynucleotides (ODNs),[5] for example, has provided an elegant means to enhance detection sensitivity in DNA sequencing.

Conjugation of an anthracene donor unit to various *F*-Bodipy emitters is known to provide a family of "dyad" fluorophores with a common excitation wavelength and tunable emission wavelengths.[6] In pyrene-functionalized *F*-Bodipys, quantitative energy transfer occurs between the pyrene center and the boradiazaindacene core through the S_2 absorption band of the core.[7] Unfortunately, the pyrene substituent, introduced at the meso position, severely restricts further possibilities of functionalization with, for example, succinimidyl, maleimide, or pentafluorophenyl ester groups, suitable for biolabeling reactions. Thus, a highly attractive alternative is to introduce a high-energy donor such as ethynyl-pyrene onto the boron center, leaving the meso position available for the introduction of the anchoring function. Herein, we describe the promising results of our efforts to synthesize a range of novel tandem-dyes bearing two ethynyl-aryl moieties linked to the boron atom and for which we suggest the designation *E*-Bodipy (*E* = ethynyl in Chart 1).

Results and Discussion

Substitution of phenyl for fluorine in *F*-Bodipy species is readily achieved using aryl-Grignard reagents in anhydrous THF,[8] similar reactions of β-diketoniminato-boron fluorides also being effective.[9] Organolithium reagents are commonly used for complete substitution on trigonal boron as in BCl_3, the resulting BR_3 compounds being stabilized by adduct formation with Lewis bases such as pyridine, triphenylphosphane, or THF.[10] As in the pioneering studies of the synthesis of tris-(acetylide)boranes stabilized by N-donors,[11] most alkynylboranes have been obtained by the reaction of lithium acetylides on their halogenoborane analogues. The precipitation of lithium halogenides is possibly the driving force for such reactions,[12] the lattice energy for instance of LiF being particularly high.[13]

Thus, to establish a procedure for the synthesis of *E*-Bodipy dyads, we first examined the reaction of lithium tolylacetylide with the simple "model" *F*-Bodipy **1** in anhydrous THF at room temperature. The reaction takes place rapidly and can be quenched with water after the disappearance of the starting compound, giving the *E*-Bodipy **2** in a reproducible yield ~70%. A variety of lithium acetylides were prepared by the titration of the appropriate functionalized ethynes with *n*-butyllithium at −78 °C and by allowing the reaction to be completed at room temperature for 5−30 min (Scheme 1). In all cases, the reaction was very fast, but increasing the size of the ethynylaryl reagent decreased the yield of the disubstituted compounds. In no case, however, was any monosubstituted product obtained.

Following these procedures, we obtained the family of new *E*-Bodipy dyads shown in Chart 2. Reactions of the acetylides derived from the arylacetylenes 2-ethynylnaphthalene,[14] 1-ethynylpyrene,[15] 2-ethynyl-(9,9-dibutyl-9H)fluorene,[16] 1-ethynylperylene,[17] and 4′-ethynyl-terpyridine[18] gave the corresponding *E*-Bodipy species in the moderate to good yields indicated, the relatively poor yield of the terpyridine derivative possibly reflecting some diversion through lithiation of the imine unit.[19]

All these compounds were fully characterized by ^1H, ^{13}C, and ^{11}B NMR spectroscopy, mass spectrometry and elemental analysis. The ^1H NMR spectra exhibit "fingerprint" resonances of the boradiazaindacene unit, with singlets for the methyl

(2) "Cascatelle" designates a small cascade or waterfall. This word was frequently used in 18th century French literature and has been introduced in the scientific literature to describe an intramolecular energy transfer process (see ref 21).

(3) Forster, T. *Discuss. Faraday Soc.* **1959**, *27*, 7−21.
(4) Ju, J.; Ruan, C.; Fuller, C. W.; Glazer, A. N.; Mathies, R. A. *Proc. Natl. Acad. Sci. U.S.A.* **1995**, *92*, 4347−4351.
(5) Glazer, A. N.; Mathies, R. A. *Curr. Opin. Biotechnol.* **1997**, *8*, 94−102. Berti, L.; Xie, J.; Medintz, I. L.; Glazer, A. N.; Mathies, R. A. *Anal. Biochem.* **2001**, *292*, 188−197.
(6) Wan, C.-W.; Burghart, A.; Chen, J.; Bergström, F.; Johanson, L. B.-A.; Wolford, M. F.; Kim, T. G.; Topp, M. R.; Hochstrasser, R. M.; Burgess, K. *Chem.−Eur. J.* **2003**, *9*, 4430−4441.
(7) Ziessel, R.; Goze, C.; Ulrich, G.; Césario, M.; Retailleau, P.; Harriman, A.; Rostron, J. P. *Chem.−Eur. J.* **2005**, *11*, 7366−7378.
(8) Murase, S.; Tominaga, T.; Kohama, A. Eur. Patent EP 1253151a1, 25.04.2002.
(9) Qian, B.; Baek S. W.; Smith, M. R., III. *Polyhedron* **1999**, *18*, 2405−2414.
(10) Bayer, M. J.; Pritzkow, H.; Siebert, W. *Eur. J. Inorg. Chem.* **2002**, 2069−2072.
(11) Ashby, E. C.; Foster W. E. *J. Org. Chem.* **1964**, *29*, 3225−3229. Soulié, J.; Cadiot, P. *Bull. Chem. Soc. Fr.* **1966**, 3846−3849.
(12) Feulner, H.; Metzler, N.; Nöth, H. *J. Organomet. Chem.* **1995**, *489*, 51−62. Davie, J. E.; Raithby, P. R.; Snaith, R.; Wheatley, A. E. H. *Chem. Commun.* **1997**, 1797−1798. Ashe, A. J., III; Bajko, Z.; Carr, M. D.; Kampf, J. W. *Organometallics* **2003**, *22*, 910−912.
(13) Stokes, R. H. *J. Am. Chem. Soc.* **1964**, *86*, 982−986.
(14) Gangjee, A.; Yu, J.; Kisliuk, R. L. *J. of Heterocycl. Chem.* **2002**, *39*, 833−840.
(15) Crisp, G. T.; Jiang, Y.-L *Synth. Commun.* **1998**, *28*, 2571−2576.
(16) Prepared by an adapted procedure from Thomas, K. R. J.; Lin, J. T.; Lin, Y.-Y.; Tsai, C.; Sun, S.-S. *Organometallics* **2001**, *20*, 2262−2269.
(17) Inouye M.; Hyodo, Y.; Nakazumi, H. *J. Org. Chem.* **1999**, *64*, 2704.
(18) Grosshenny, V.; Romero, F. M. Ziessel, R. *J. Org. Chem.* **1997**, *62*, 1491−1500.
(19) Similar reactivity to previous described lithiopyridine, quinoline, or bipyridine derivatives; see: (a) Zoltewicz, J. A.; Dill, C. D. *Tetrahedron* **1996**, *52*, 14469−14474. (b) Gros, P.; Fort, Y.; Caubère, P. *J. Chem. Soc., Perkin Trans. 1* **1997**, 3597−3600.

CHART 2

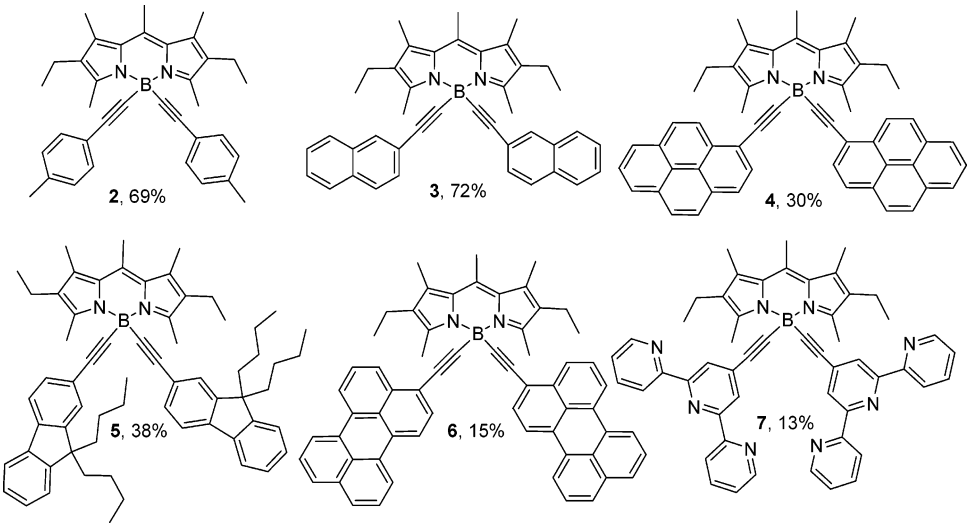

TABLE 1. Selected Spectroscopic Data for the *E*-Bodipy Dyads

compds	^{1}H NMR[a]	^{11}B NMR[a]	IR $\nu_{c\equiv c}$[b]
2	2.84	−9.69	2173
3	2.93	−9.63	2172
4	3.11	−9.17	2167
5	2.96	−9.60	2172
6	3.00	−9.40	2172
7	2.84	−9.88	n.o.
9a	3.21	−8.72	2161
9b	3.21	−8.91	2169
9c	3.15	−8.92	2164
11	3.16	−8.94	2169
12	3.15	−8.97	2165
13	3.14	−8.92	2164
15	3.14	−8.92	2172

[a] In $CDCl_3$, rt, chemical shifts of 3,5-dimethyl groups in ppm; for ^{11}B, chemical shifts are relative to residual glass borate. [b] KBr pellets, C≡C stretching vibrations in cm^{-1}; n.o. = not observed.

groups adjacent to N appearing at δ 2.49 for **1**, 2.84 for **2**, and 3.21 for **9b** (Table 1). A ^{13}C resonance for the acetylide carbon atoms directly bound to boron is not seen under normal experimental conditions because of coupling with the quadrupolar boron nucleus[20a,b] but the other acetylide carbon resonances appear in the δ 90−95 range. The triplet, reflecting coupling to two equivalent fluorine nuclei, seen near δ 3.8 in the ^{11}B NMR spectra of **1**, **8a**−**c** and **10** becomes a singlet at $\delta \sim -9.5$ in dyads **2**−**6**, **9a**−**c**, and **10**−**14**, this strong shielding indicates that the boron lies in the shielding cone of the ethyne bond (Table 1). A weak band attributed to the C≡C stretching vibration is observed at 2160 to 2180 cm^{-1} in FT-IR spectra.[20c]

All these new compounds are very stable and insensitive to strong base or acid, as well as polar solvents and reagents. This robustness is probably due to stabilization of the tetrahedral boron center by the ethynyl donors.

In our earlier work on pyrene-based dyads, the pyrene units were attached to the pseudo-meso position of *F*-Bodipy derivatives.[6] The present studies have shown that additional pyrene units can be introduced through pyreneacetylide substituents on boron, the substitution reactions being acceptably efficient even

SCHEME 2 [a]

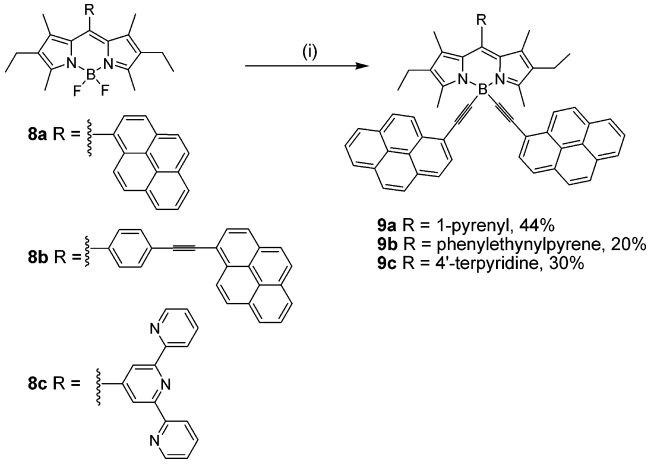

[a] Keys: (i) 1-Lithioethynylpyrene (2 equiv), THF, rt, 5−15 min.

when large substituents such as pyrene (giving dyads **9a** and **9b** with three pyrene antennae) and terpyridine (dyad **9c**) are already present on the meso position (Scheme 2).

To evaluate Bodipy-based dyads as biological labels, it is essential to introduce functionality enabling their grafting to biomolecules and to show that this functionality is not deleterious to their spectroscopic properties.[21] Our choice of grafting group was a succinimidyl unit, known to react readily with protein side chain amino groups such as those from lysine. This was attached through reactions (Scheme 3) of an *F*-Bodipy bearing an iodophenyl substituent at the meso position, this substituent being selected because of its low reactivity toward alkali-metal alkynes but ready involvement in d^8-transition-metal-catalyzed cross-coupling reactions. After some experimentation, we were pleased to find that *F*-Bodipy **10**[22] was efficiently converted (70%) to the corresponding *E*-Bodipy **11** following the standard procedure described above. In an additional step, a Sonogashira cross-coupling reaction with 1

(20) (a) Wrackmeyer, B.; Nöth, H. *Chem. Ber*. **1977**, *110*, 1086−1094. (b) Yamamoto, Y.; Moritani, I. *J. Org. Chem.* **1975**, *40*, 3434−3437. (c) Köster, R.; Horstschäfer, H.-J.; Binger, P. *Justus Liebigs Ann. Chem.* **1968**, *717*, 1−20.

(21) Ulrich, G.; Goze, C.; Guardigli, M.; Roda, A.; Ziessel, R. *Angew. Chem., Int. Ed*. **2005**, *44*, 3695−3698.

(22) Burghart, A.; Kim. H.; Wech, M. B.; Thorensen, L. H.; Reibenspies, J.; Burgess, K. *J. Org. Chem*. **1999**, *64*, 7813−7819.

SCHEME 3 [a]

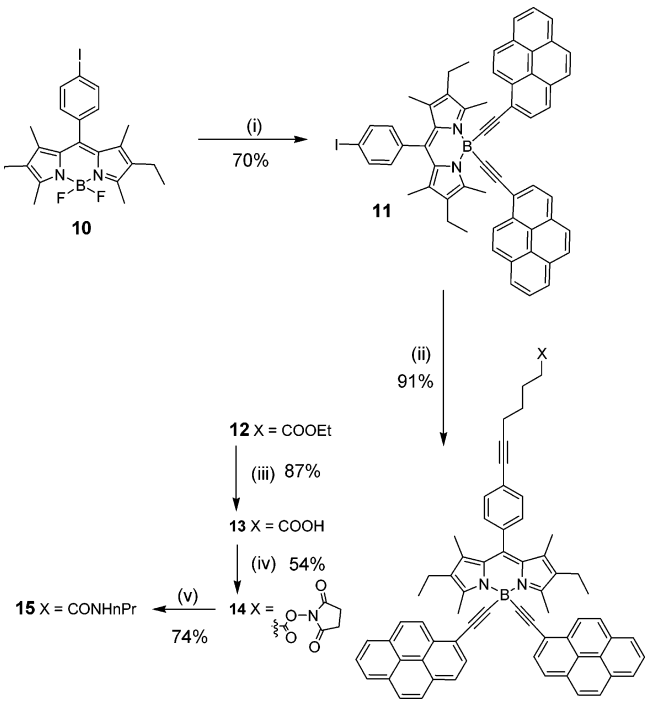

[a] Keys: (i) 1-Lithioethynylpyrene (2 equiv), THF, rt, 15 min; (ii) $HC{\equiv}C(CH_2)_4COOEt$ (1 equiv), $[Pd(PPh_3)_2Cl_2]$ (6% mol), CuI (10% mol), THF/*i*-Pr_2NH, rt, 16 h; (iii) NaOH (10 equiv), EtOH/THF (1:1), 60 °C, 12 h; (iv) DMAP (2 equiv), EDCI (2 equiv) NHS (2 equiv), rt, 1 h; (v) *n*-$PrNH_2$, rt, 1 h.

equiv of ethyl hept-6-ynoate and compound **11** mediated by catalytic amounts of Pd^{II} and Cu^{I} gave the ester **12** in good yield. After saponification of the ester groups with a strong base, the corresponding carboxylic acid **13** was converted to the active succinimidyl ester **14** (54%) by the use of an EDCI/DMAP coupling and *N*-hydroxysuccinimide.

The high reactivity of this activated ester **14** toward amino groups was confirmed by a reaction with *n*-propylamine as a model compound, providing the amido derivative **15** in fair yield. This compound is considered as a model analogue of labeled proteins and its photophysical properties revealed that the intramolecular energy transfer in our cascatelle is still very effective (vide infra).

X-ray Structure Analysis

Single-crystal X-ray structures were obtained for compounds **2** and **4**. The molecular units are shown in Figures 1 and 2, respectively.

In both structures, the boron atom has a distorted tetrahedral environment. Typical bond angles are 105.9 (2)° for N−B−N and 114.7 (2)° for C−B−C in **2** and 105.9 (2)° and 111.6 (4)° respectively for **4**. The average B−N bond length is 1.562 (2) Å, slightly longer than what is observed in *F*-bodipy.[23] The average N1−C1/N2−C17 bond length is 1.349(4) Å, consistent with double bond localization here, as reflected also in the longer bond length of 1.402 (1) Å for C8−N1/C11N2. Both values are comparable to those found in *F*-Bodipy analogues.[6,7,22,23] The elongated B−C bonds in **2** and **4**, average length of 1.593 (7) Å, are similar to those found in a tris(alkynyl)borane pyridine adduct.[10] The triple bond character of the ethyne link appears to be maintained, with a bond length of 1.20(1) Å. In **4**, the boron center is displaced from the mean plane of the diazaindacene by 0.109 Å, while in **2** there is no significant displacement (0.023 Å). The central six-membered ring lies coplanar with the adjacent five-membered ring [the maximum deviation from the least-squares mean plane for the 12 atoms of the indacene group being ca. 1.5° for **2** and ca. 3.7° for **4**].

Electrochemical Properties

An investigation of the extent of electronic interactions between the various subunits and the impact of the dialkynylboron module in these novel dyad molecules was based on cyclic voltammetry in dichloromethane. The electrochemical data for the *E*-Bodipy molecules and some reference compounds **A**, **B**, and **C** are gathered in Table 2. The prototypical *F*-Bodipy **1** displays a one-electron reversible oxidation wave at +0.95 V and a one-electron reversible reduction wave at −1.43 V versus SCE. In the *E*-Bodipy compounds **2** and **3**, the cycles remain reversible but the oxidations become more facile by 110 and 80 mV, respectively, while the reductions become less ready by 110 and 150 mV, respectively (Figure 3).

Unlike certain pyridine Bodipy adducts,[25] there is no indication of oxidation to the ($Bodipy^{2+}$) dication or reduction to the ($Bodipy^{2-}$) dianion within the given electrochemical window. On changing the aromatic fragments from tolyl to naphthyl, to pyrenyl, to fluorenyl, or to perylenyl, the *E*-Bodipy oxidations and reductions lie within the same range (+0.82 to +0.89 V for the $Bodipy^{+\bullet}$ and −1.52 to −1.59 V for the $Bodipy^{-\bullet}$, Figure 4). However, for compounds **4**, **5**, and **6**, additional processes are observed and assigned with respect to reference compounds **A**, **B**, and **C** (Chart 3). Interestingly, the protected ethynylfluorene **B** is more difficult to oxidize (by 180 mV) than the ethynylpyrene **A** or ethynylperylene **C** (by 310 mV). It is also apparent that attachment of the boradiazaindacene entity facilitates oxidation of these units. Thus, comparison of the results for **4**, **5**, and **6** and the reference compounds shows that oxidation is easier by 140 mV for the fluorene, 220 mV for the pyrene, and 460 mV for the perylene derivatives. This observation is in line with the increase of electron density imported by the Bodipy fragment and the ability of the polyaromatic ethynylboron to stabilize the radical cation. In the case of compound **6**, an additional, reversible wave is attributed to the reduction of the perylene nucleus. This process is irreversible in the fluorene case (Table 2). For the pyrene compound **4**, no additional redox processes could be detected in the +1.6 to −2.2 V window.

By replacing ethynylpyrene in **4** by ethynyl-terpyridine in **7** a weak cathodic shift (−30 mV) of the monoelectronic oxidation and a weak anodic shift (+50 mV) of the reduction of the Bodipy fragment is found. As in the case of the perylene derivative, for compound **6** an additional reversible dielectronic wave is observed at negative potentials. This is probably due to the reduction of both terpyridine subunits.[25] However, a fortuitous overlap of two single electron processes, one localized on a terpyridine and the second on the indacene, cannot be completely excluded at this stage.

(23) Shen, Z.; Röhr, H.; Rurack, K.; Uno, H.; Spieles, M.; Schulz, B.; Reck, G.; Ono, N. *Chem.—Eur. J.* **2004**, *10*, 4853−4871.

(24) Ulrich, G.; Ziessel, R. *J. Org. Chem.* **2004**, *69*, 2070−2083.

(25) Karolin, J.; Johansson, L. B.-A.; Strandberg, L.; Ny, T. *J. Am. Chem. Soc.* **1994**, *116*, 7801−7806.

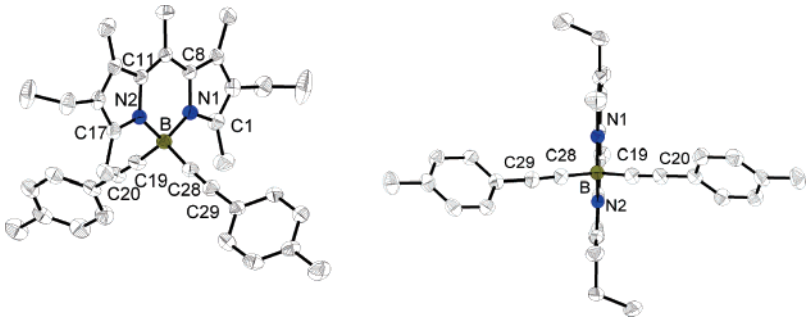

FIGURE 1. ORTEP views of compound **2** (displacement ellipsoids at the 50% probability level).

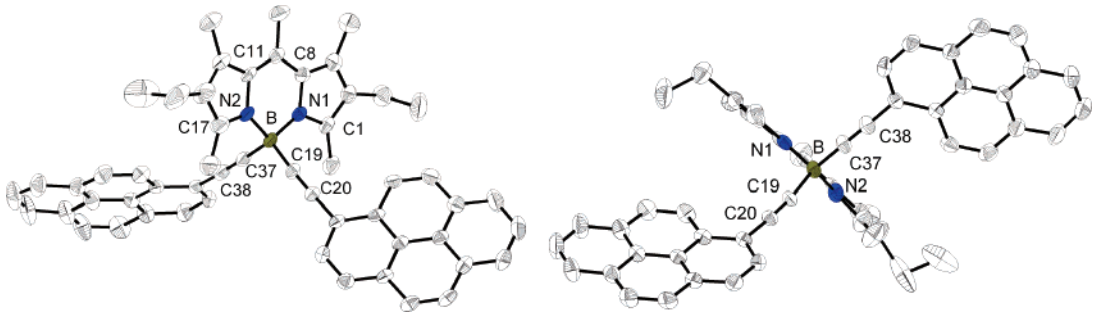

FIGURE 2. ORTEP views of compound **4** (displacement ellipsoids at the 50% probability level).

TABLE 2. Solution Electrochemical Properties of the Bodipy−Pyrene Dyes and Appropriate Reference Compound[a]

	E^{i0}_{ox}, V (ΔE, mV)		E^{i0}_{ox}, V (ΔE, mV)	
compd	aryl$^{+\bullet}$/aryl	Bodipy$^{+\bullet}$/Bodipy	Bodipy/Bodipy$^{-\bullet}$	aryl/aryl$^{-\bullet}$
1		+0.95 (70)	−1.43 (60)	
2		+0.84 (70)	−1.55 (70)	
3		+0.87 (70)	−1.58 (70)	
A	+1.52 (irrev, $I_c/I_a \approx 0.3$)			
4	+1.30 (irrev, $I_c/I_a \approx 0.2$)	+0.89 (60)	−1.52 (60)	
B	+1.70(irrev, $I_c/I_a \approx 0.1$)			
5	+1.56(irrev, $I_c/I_a \approx 0.2$)	+0.86 (60)	−1.59 (60)	
C	+1.39(irrev, $I_c/I_a \approx 0.2$)			−1.93 (irrev, $I_a/I_c \approx 0.3$)
6	+0.93(irrev, $I_c/I_a \approx 0.2$)	+0.82 (60)	−1.56 (60)	−1.80 (80)[b]
7		+0.86 (60)	−1.47 (70)	−1.86 (80)
8a	+1.48 (60)	+1.02 (60)	−1.29 (70)	−1.96(70)
8b	+1.28 (60)	+0.99 (70)	−1.32 (80)	−1.68 (80)
9a	+1.31 (irrev, $I_c/I_a \approx 0.2$)	+0.92 (70)	−1.45 (80)	−2.06 (70)
9b	+1.32 (irrev, $I_c/I_a \approx 0.2$)	+0.90 (70)	−1.44 (60)	−1.78 (80)
9c	+1.30 (irrev, $I_c/I_a \approx 0.2$)	+0.83 (60)	−1.47 (70)	−1.72 (80)
10	+1.42 (irrev, $I_c/I_a \approx 0.3$)	+1.10 (60)	−1.27 (60)	
11	+1.33 (irrev, $I_c/I_a \approx 0.1$)	+0.95 (70)	−1.46 (80)	
12	+1.33 (irrev, $I_c/I_a \approx 0.2$)	+0.93 (70)	−1.49 (80)	
13	+1.32 (irrev, $I_c/I_a \approx 0.2$)	+0.92 (70)	−1.47 (60)	
15	+1.32 (irrev, $I_c/I_a \approx 0.2$)	+0.93 (70)	−1.46 (60)	

[a] Potentials determined by cyclic voltammetry in deoxygenated CH_2Cl_2 solution, containing 0.1 M $TBAPF_6$, at a solute concentration of ca. 1 mM and at 20 °C. Potentials were standardized versus ferrocene (Fc) as internal reference and converted to the SCE scale assuming that $E_{1/2}$ (Fc/Fc$^+$) = +0.38 V (ΔE_p = 70 mV) vs SCE. Error in half-wave potentials is ±10 mV. Where the redox process is irreversible, the peak potential (E_{ap}) is quoted, and the relative peak heights are given as I_a/I_c. All reversible redox steps result from one-electron processes unless otherwise specified. [b] Two-electron process.

The rich voltammetry exhibited by derivatives **9a**,**b** bearing an additional pyrene fragment attached at the meso position can be understood in light of the previously reported redox behavior of compounds **8a**,**b**.[7] First, as for **2** and **3**, the substitution of fluoro ligands by ethynylpyrene renders the Bodipy easier to oxidize by ca. 100 mV and more difficult to reduce by ca. 150 mV. However, the HOMO/LUMO gap remains essentially the same (about 2.3 eV), as reflected by the constancy of the emission wavelength (vide infra). In contrast with the fluoro derivatives, the oxidation of all the pyrene residues becomes irreversible and less anodic, whereas the reduction of the Bodipy core to the radical anion remains reversible and cathodically shifted by 160 mV in **9a** compared to **8a** and by 120 mV in **9b** compared to **8b**. Interestingly, an additional reversible monoelectronic process, absent in compound **4**, may signify reduction of the appended pyrene units present in the meso position. The difference in half-wave potentials between compounds **9a**,**b** and **8a**,**b** is probably a consequence of electrostatic effects. The presence of a phenylethynyl appendage in **9b** facilitates the reduction of the pyrene center by 280 mV with respect to compound **9a**, a result in keeping with the redox activity of compound **8b**. These observations reflect the different electronic environments of Bodipy and pyrene groups and indicate that significant electronic interactions occur despite the quasi-

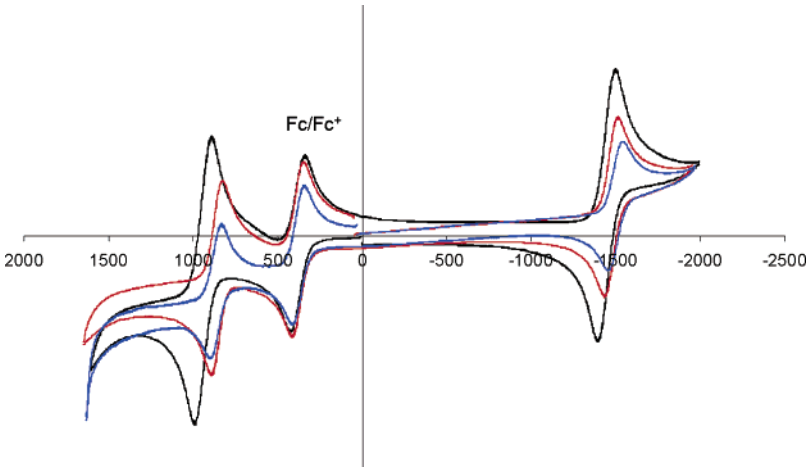

FIGURE 3. Cyclic voltammograms of **1** (black), **2** (red), and **3** (blue) measured in CH_2Cl_2 solution, containing 0.1 M $TBAPF_6$ at 20 °C. Ferrocene (Fc) was used as internal reference, and potentials were calculated as relative to the SCE assuming that $E_{1/2}$ (Fc/Fc^+) = +0.38 V (ΔE_p = 70 mV) vs SCE.

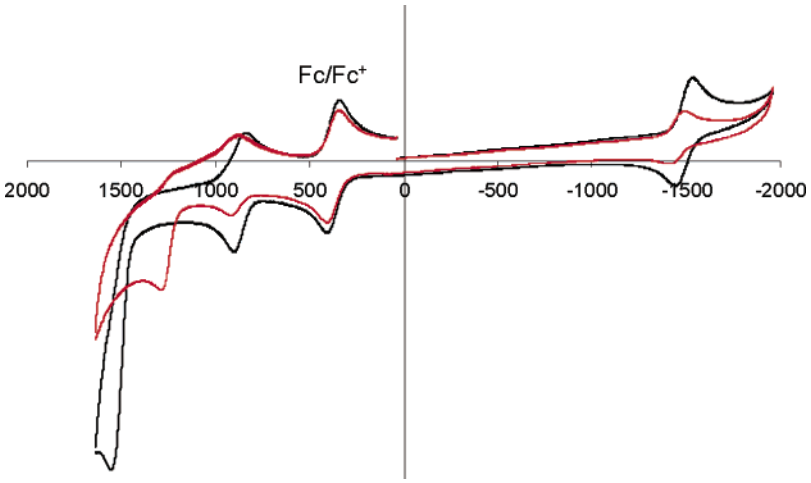

FIGURE 4. Cyclic voltammogram of **5** (black) and **4** (red), measured in CH_2Cl_2 solution, containing 0.1 M $TBAPF_6$ at 20 °C. Ferrocene (Fc) was used as internal reference and potentials calculated as relative to the SCE assuming that $E_{1/2}$ (Fc/Fc^+) = +0.38 V (ΔE_p = 70 mV) vs SCE.

CHART 3

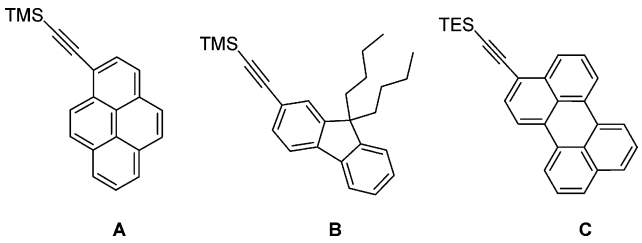

orthogonality of the Bodipy and phenyl fragments, as found in related derivatives. These results clearly reflect the combined effects of electron withdrawal and charge delocalization and are in keeping with previous observations on related molecules.[7]

Another interesting situation is found for compound **9c**. Replacement of the methyl group in the meso position by a terpyridine fragment results in the easier oxidation (by 60 mV) and easier reduction (by 50 mV) of the Bodipy fragment compared with compound **4** (Table 2). Here, there is also an additional one-electron reduction step occurring at strongly cathodic potentials. This extra step is presumed to involve attachment of an electron to the appended terpyridine unit. Again, this is probably a consequence of extended electron-delocalization at the π-radical cation and anion stage. Notably, the replacement of the terpyridine unit in **9c** by pyrene-substituted derivatives shifts the oxidation of the Bodipy anodically by 70 mV while the reduction remains almost unchanged at −1.46 V. When compared to data recorded for the reference compound **10**, it appears that substitution of pyrenylethynyl units for fluorine facilitates oxidation but hampers reduction (Figure 5).

Finally, the introduction of ethynyl groups in place of iodo as in compounds **12**, **13**, and **15** has little influence on the redox activity of the indacene core and the pyrene subunits. Apparently, there is no very effective transmission of the electronic influence of groups attached to the meso position of the Bodipy unit.

Optical Properties

Spectroscopic data relevant to the present discussion are collected in Table 3. In solution, all the compounds show a strong $S_0 \rightarrow S_1$ ($\pi-\pi^*$) transition between $\lambda \approx 516-528$ nm with an absorption coefficient of 50 000−80 000 $M^{-1}cm^{-1}$, unambiguously assigned to the boradiazaindacene chromophore.

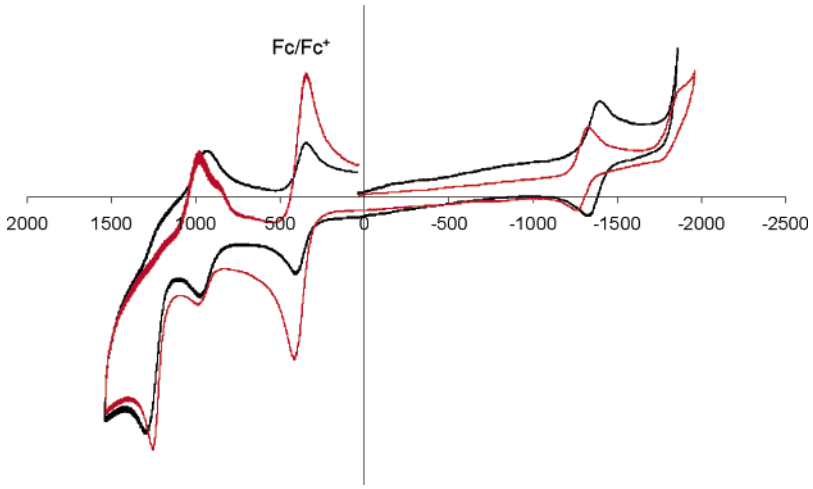

FIGURE 5. Cyclic voltamogramm of **10** (black) and **9c** (red), measured in CH_2Cl_2 solution, containing 0.1 M $TBAPF_6$ at 20 °C. Ferrocene (Fc) was used as internal reference and potentials calculated as relative to the SCE assuming that $E_{1/2}$ (Fc/Fc^+) = +0.38 V (ΔE_p = 70 mV) vs SCE.

TABLE 3. Spectroscopic Data for the Compounds at 298 K[a]

compds	λ_{abs} (nm)	ϵ (M^{-1} cm^{-1})	λ_F (nm)	Φ_F[b]	P_{ET}[c]	τ_F (ns)	k_r[d] (10^8 s^{-1})	k_{nr}[d] (10^6 s^{-1})	Stokes' shift (cm^{-1})	ΔG_{ES} eV[e]	$E°_{B*/B+\cdot}$ eV[f]	$E°_{B-\cdot/B*}$ eV[g]
1	517	64 500	538	83		6.2	1.34	27.39	755	2.43	−1.48	1.00
2	516	67 100	537	95		9.0	1.06	5.60	758	2.44	−1.60	0.89
3	517	78 000	537	90	36	9.5	0.95	10.53	720	2.45	−1.58	0.87
	284	27 500	537	32					16 600			
4	516	73 000	535	94	96	6.2	1.52	9.68	690	2.43	−1.54	0.91
	371	95 000	535	90					8 260			
5	517	70 000	535	95	95	9.5	1.00	5.26	650	2.45	−1.59	0.86
	323	80 000	535	90					12 300			
6	516	63 200	535	94	99	7.6	1.24	7.89	688	2.45	−1.63	0.89
	464	97 000	535	93					2 860			
7	516	61 000	536	80		6.8	1.18	29.41	723	2.44	−1.58	0.97
9a	525	84 000	540	95	97	4.0	2.38	1.25	530	2.40	−1.48	0.95
	369	111 000	540	92					8 600			
9b	528	70 000	540	98	99	5.4	1.81	3.70	420	2.40	−1.50	0.96
	368	138 400	540	97					8 650			
9c	525	70 000	590	40	100	6.6	0.61	90.90	1 990	2.40	−1.57	0.93
	369	100 000	590	40					10 150			
11	522	70 000	538	80	98	5.7	1.40	35.09	570	2.43	−1.48	0.97
	371	72 500	538	78					8 400			
12	522	50 000	536	90	95	6.2	1.45	16.13	500	2.42	−1.49	0.93
	374	62 000	536	85					8 080			
13	522	60 000	537	80	100	6.3	1.27	31.75	535	2.42	−1.50	0.95
	373	75 000	537	80					8 200			
14	522	55 000	538	90	100	5.4	1.7	17	570	2.43	/	/
	372	70 000	538	82					8 300			
15	522	61 000	538	82	67	5.0	1.6	36	570	2.40	−1.47	0.94
	370	88 000	538	55					8 450			

[a] Determined in dichloromethane solution. [b] Determined in dichloromethane solution, ca. 5×10^{-7} M. Using Rhodamine 6G, as reference Φ = 0.78 in water, λ_{exc} = 488 nm.[27] All Φ_F are corrected for changes in refractive index. [c] Energy transfer efficiency calculated by dividing the photoluminescence quantum yield obtained by irradiation in the aryl fragment by the yield obtained by direct excitation in the S_1 transition. [d] Calculated using the following equations: $k_r = \Phi_F/\tau_F$, $k_{nr} = (1 - \Phi_F)/\tau_F$, assuming that the emitting state is produced with unit quantum efficiency. [e] Excited-state energies were estimated (±5%) by drawing a tangent on the high energy side of the emission. [f] Calculated excited-state oxidation potential vs SCE, $E°(B^+/B^*) = E°(B^+/B) - \Delta G_{ES}$; B = Bodipy) Calculated excited-state reduction potential vs SCE, $E°(B^*/B^{-\cdot}) = E°(B/B^{-\cdot}) + \Delta G_{ES}$. For the reactive ester **14**, the electrochemical data are not available.

For the model compound **2**, the weak and broad band located at $\lambda \approx 375$ nm is attributed to the $S_0 \rightarrow S_2$ ($\pi-\pi^*$) transition[25] of the boradiazaindacene (Figure 6). Another weak band at ca. 316 nm is attributed to the $\pi-\pi^*$ transition of the ethynyl bond.[26] For the polyaromatic fragments, strong $\pi-\pi^*$ transitions with marked vibronic structure are observed at 275−320 nm for naphthalene, 320−370 and 230−310 nm for pyrene, 250−340 nm for fluorene, and 400−480 nm for perylene (Figure 7). In the dyad systems with pyrene and perylene antenna, the weak transitions (S_2 and $\pi-\pi^*$) overlap the strong $\pi-\pi^*$ absorptions of the polyaromatic nuclei. The absorption spectra of compounds **3**−**9b** and **11**−**15** can be analyzed as superpositions of the separate absorptions of the boradiazaindacene and the polyaromatic fragments, confirming the absence of electronic delocalization through the boron connection.

(26) Masai, H.; Sonogashira, K.; Hagihara, N. *Bull. Chem. Soc. Jpn.* **1971**, *44*, 2226−2230.

(27) Olmsted, J., III. *J. Phys. Chem.* **1979**, *83*, 2581−2584.

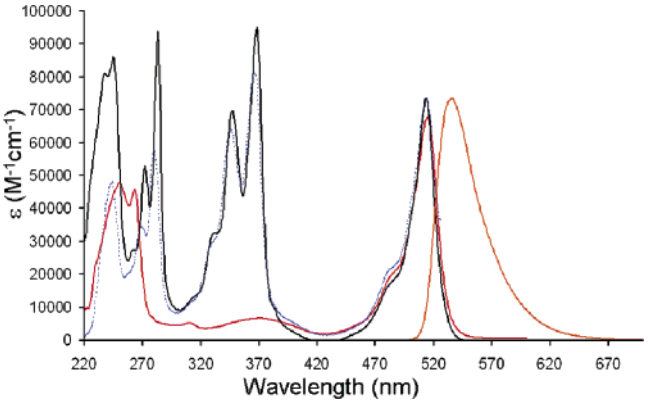

FIGURE 6. Absorption spectra of **2** (red line) and **4** (black line), excitation spectrum of **4** (dotted blue line), and the common emission spectrum for both dyes (orange line).

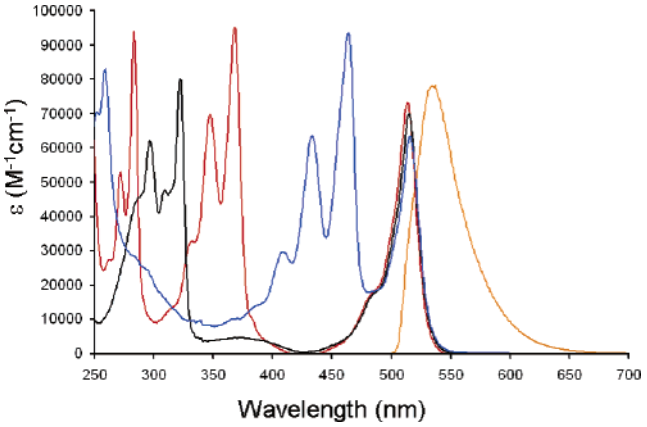

FIGURE 7. Absorption spectra of **4** (red line), **5** (black line), and **6** (blue line) and the common emission spectrum (orange line).

For all the new compounds, excitation in the 516−528 nm band ($S_0 \rightarrow S_1$ transition), leads to a strong emission in the region 535−540 nm, with high quantum yields in the 80 to 98% range, typical of Bodipy frameworks (Table 3). The fluorescence spectrum shows good mirror symmetry with the lowest energy absorption transition (Figures 6−8), confirming that these transitions are due to the same state and typical of singlet emitters. Furthermore, the fluorescence decay profiles can be described by a single-exponential fit, with fluorescence lifetimes in the range of 1−10 nanoseconds, in accordance with a singlet excited state. In fact, most of the radiative rate constants (about 10^8 s^{-1}) are much faster than the nonradiative rate constants (about 10^6 s^{-1}), indicating minimal interaction of the emitting state with an energetically low lying localized state (triplet or charge transfer states) reflected in the high quantum yields. At this stage of our investigations, we do not have any evidence for the formation of a triplet excited state. In addition, no significant solvatochromic effect was observed in the absorption and fluorescence spectra, confirming weak polarization of the ground and excited states which is also in keeping with a singlet excited state.

For compounds **3**−**6**, **9a**,**b**, and **11**−**15**, excitation in the most intense absorption band of the polyaromatic fragments (250−470 nm range), did not lead to the emission of the polycyclic fragments but to the characteristic emission of the boradiazaindacene core. In all cases, the fluorescence excitation spectra match the absorption spectra, confirming a very efficient energy transfer from the polyaromatic parts to the indacene emitter. The quantum yield measurements are in agreement with an efficiency of 95−100% for this transfer, except for **3** possessing a naphthalene unit. The efficiency of the energy transfer is due to a good overlap of the $S_0 \rightarrow S_2$ band of the boradiazaindacene emitter with the emission band of, for example, the pyrene unit leading to a very efficient Förster type energy transfer, as we previously observed with a meso-substituted pyrene−Bodipy dyad.[7] For the perylene derivative **6**, a strong overlap between the emission of the perylene and the $S_0 \rightarrow S_1$ absorption band of the boradiazaindacene is responsible for the almost quantitative energy transfer. However, for the naphthyl dye **3**, the efficiency of energy transfer drops to 36% owing to a poor spectral overlap.

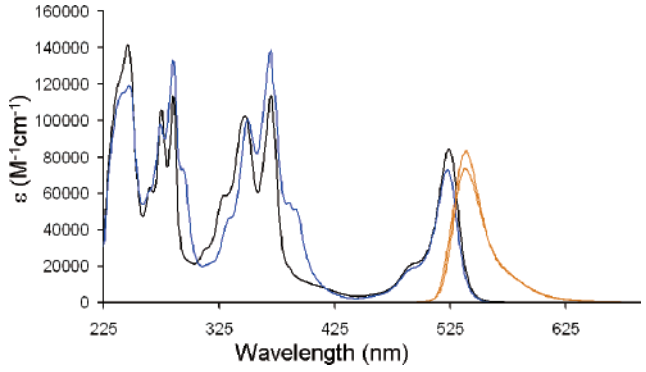

FIGURE 8. Absorption spectra of **9a** (black line) and **9b** (blue line) and the common emission spectra (orange lines).

Concerning the polypyrene antenna compounds **9a**,**b** (Figure 8), bearing three appended pyrene moieties, a very high molar extinction coefficient in the 350−380 nm region is obtained. The lower-energy vibronic band observed near 400 nm for compound **9b** is due to the phenyl−ethynyl−pyrene spacer linked to the pseudo-meso position. The high energy transfer efficiency observed in both cases (>98%), indicates an almost quantitative transfer from all the pyrenes surrounding the Bodipy center.

Furthermore, for compound **15** (considered as a model for labeling of a protein such as bovine serum albumin),[21] the fluorescence efficiency is only slightly affected by the presence of an amido group. Also, energy transfer from the pyrene units to the Bodipy chromophore remains effective (67%), with a virtual Stokes' shift of about 8500 cm^{-1}. These particular properties observed for the model compound **15** are auspicious for the use of such dyads for biomolecule labeling.

Finally, all excited-state energies lie in the 2.40 to 2.45 eV range; the use of the first reduction and oxidation potentials (from Table 2) allows the calculation of the redox potential of the first excited state and the conclusion that this excited state is a strong reductant but a modest oxidant (Table 3).

Concluding Remarks

The introduction of functionalized ethynyl groups on the boron center of boradiazaindacene opens the way to a new class of highly luminescent dyes. The easy grafting of a supplementary chromophore leads to tandem devices in which excitation of the polyaromatic nucleus results in almost quantitative intramolecular energy transfer to the emitting dyes, incidentally

providing large virtual Stokes' shifts. Thus, new cascatelle devices with tunable absorptions spanning over 250 nm from 270 to 520 nm have been engineered. The new family of molecules displays intriguing optical properties including high absorption coefficient, high quantum yields, and relatively narrow emission bands. When needed, an activated functional group (e.g., a succinimidyl ester) can be easily introduced in the meso position of the dipyrromethene core.

Both radical cation and radical anion species are readily generated from the new dyads. The potentials required are shifted by ~100 mV from those of their *F*-Bodipy analogues, though the HOMO/LUMO gap is similar for all molecules. Modulation of this gap could be significant for optoelectronic applications and work toward this objective is in progress.

Experimental Section

General Procedure for the Substitution of Fluoride by Acetylide. In a Schlenk flask, *n*-butyllithium (2.2 equiv) was added at −78 °C, to a stirred degassed solution of the acetylenic compound (2.2 equiv) in anhydrous THF or diethyl ether. The mixture was stirred at −78 °C for 1 h and at room temperature for 30 min. The resulting anion was then transferred via cannula to a degassed solution of the precursor difluoroboradiazaindacene (1 equiv) in anhydrous THF (or diethyl ether). The solution was stirred at room temperature until the complete consumption of the starting material was observed by TLC. Water was added, and the solution was extracted with CH_2Cl_2. After evaporation, the organic layer was purified by column chromatography and recrystallized from CH_2Cl_2/hexane.

4,4-Bis(2-naphthylethynyl)-1,3,5,7,8-pentamethyl-2,6-diethyl-4-bora-3a,4a-diaza-*s*-indacene (3). Prepared according to the general procedure with 2-ethynylnaphthalene (0.096 g, 0.62 mmol) in 10 mL of THF, 0.44 mL of *n*-butyllithium (1.55 M in *n*-hexane), and **1** (0.1 g, 0.31 mmol) in 20 mL of THF. Complete consumption of the starting material was observed after 5 min. The chromatography was performed on alumina (CH_2Cl_2/cyclohexane, 10:90), and recrystallization gave 0.132 g of **3** (72% yield). ^{1}H NMR ($CDCl_3$ 300 MHz): δ = 7.89 (s, 2H), 7.77−7.68 (m, 6H), 7.49−7.40 (m, 6H), 2.93 (s, 6H), 2.67 (s, 3H), 2.50 (q, 4H, ^3J = 7.5 Hz), 2.39 (s, 6H), 1.12 (t, 6H, ^3J = 7.5 Hz). ^{13}C {^{1}H} NMR ($CDCl_3$, 75 MHz): 152.1, 139.8, 134.6, 133.2, 132.7, 132.4, 130.9, 130.3, 129.2, 127.7, 127.6, 127.5, 126.2, 125.9, 123.1, 17.6, 17.4, 15.2, 14.8, 14.2. ^{11}B {^{1}H} NMR ($CDCl_3$, 128 MHz): −9.63 (s). UV−vis (CH_2Cl_2) λ nm (ϵ, M^{-1} cm^{-1}): 517 (77 700), 303 (29 900), 292 (34 500), 284 (27 300), 255 (110 000), 246 (97 500). IR (KBr): ν = 3413 (s), 2961 (s), 2172 (s), 1554 (s), 1184 (s), 1184 (s), 978 (s). FAB$^+$ *m*/*z* (nature of peak, relative intensity): 583.1 ([M + H]$^+$, 100), 431.2 ([M−naphtha−≡−]$^+$, 15). Anal. Calcd for $C_{42}H_{39}BN_2$: C, 86.59; H, 6.75; N, 4.81. Found: C, 86.32; H, 6.52; N, 4.62.

4,4-Bis(9,9-dibutyl-9*H*-fluorene-2-ethynyl)-1,3,5,7,8-pentamethyl-2,6-diethyl-4-bora-3a,4a-diaza-*s*-indacene (5). Prepared according to the general procedure with 2-ethynyl-9,9-dibutylfluorene (0.095 g, 0.31 mmol) in 10 mL of THF, 0.18 mL of *n*-butyllithium (1.74 M in *n*-hexane), and **1** (0.05 g, 0.16 mmol) in 10 mL of THF. Complete consumption of the starting material was observed after 15 min. The chromatography was performed on silica (CH_2Cl_2/cyclohexane, 20:80), and recrystallization gave 0.05 g of **5** (38% yield). ^{1}H NMR ($CDCl_3$, 400 MHz): δ = 7.65−7.62 (m, 2H), 7.55. (d, 2H, ^3J = 7.7 Hz), 7.39−7.26 (m, 10H), 2.96 (s, 6H), 2.67 (s, 3H), 2.52 (q, 4H, ^3J = 7.5 Hz), 2.40 (s, 6H), 1.92 (t, 8H, ^3J = 8.3 Hz), 1.14 (t, 6H, ^3J = 7.5 Hz), 1.05 (q, 8H, ^3J = 7.2 Hz), 0.6 (t, 12 H, ^3J = 7.2 Hz), 0.58−0.50 (m, 8H). ^{13}C {^{1}H} NMR ($CDCl_3$, 100 MHz):152.1, 151.0, 150.4, 141.0, 140.2, 139.8, 134.6, 132.7, 130.8, 130.3, 127.1, 126.8, 125.9, 124.1, 122.9, 119.8, 119.3, 55.0, 40.4, 26.0, 23.2, 17.7, 17.5, 15.2, 14.9, 14.3, 13.9. ^{11}B {^{1}H} NMR ($CDCl_3$, 128 MHz): −9.6 (s). UV−vis (CH_2Cl_2) λ nm (ϵ, M^{-1} cm^{-1}): 517 (70 000), 323 (80 000), 297 (62 100), 228 (38 500). IR (KBr): ν = 2959 (s), 2928 (s), 2859 (m), 2172 (m),1556 (s), 1479 (m), 1451 (m), 1324 (m), 1262 (m), 1184 (s), 1122 (m), 1028 (m), 978 (s), 800 (s), 739 (m), 715 (m). FAB$^+$ *m*/*z* (nature of peak, relative intensity): 883.1 ([M]$^+$, 100). Anal. Calcd for $C_{64}H_{75}BN_2$: C, 87.04; H, 8.56; N, 3.17. Found: C, 86.81; H, 8.36; N, 2.84.

4,4-Bis(pyrenyl-1-ethynyl-)8-(1-pyrenyl)-1,3,5,7-tetramethyl-2,6-diethyl-4-bora-3a,4a-diaza-*s*-indacene (9a). Prepared according to the general procedure with 1-ethynylpyrene (0.09 g, 0.40 mmol) in 10 mL of THF, 0.23 mL of *n*-butyllithium (1.7 M in *n*-hexane), and 4,4-difluoro-8-(-1-pyrenyl)-1,3,5,7-tetramethyl-2,4-diethyl-4-bora-3a,4a-diaza-*s*-indacene **8a** (0.1 g, 0.2 mmol) in 20 mL of THF. Complete consumption of the starting material was observed after 5 min. The chromatography was performed on alumina (CH_2Cl_2/cyclohexane, 20:80), and recrystallization gave 0.072 g of **9a** (44% yield). ^{1}H NMR ($CDCl_3$ 300 MHz): δ = 8.89 (d, 1H, ^3J = 8.9 Hz), 8.86 (d, 1H, ^3J = 9.0 Hz), 8.34−7.98 (m, 25H), 3.21 (s, 6H), 2.38 (q, 4H, ^3J = 7.5 Hz), 1.05 (t, 6H, ^3J = 7.5 Hz), 0.9 (s, 6H). ^{13}C {^{1}H} NMR ($CDCl_3$, 75 MHz): δ = 154.2, 139.1, 136.7, 133.2, 131.4, 131.2, 130.2, 129.7, 127.9, 127.8, 127.5, 127.4, 126.3, 126.0, 125.5, 125.3, 125.1, 124.9, 124.4, 120.6, 53.4, 17.5, 14.8, 14.6, 11.4. ^{11}B {^{1}H} NMR ($CDCl_3$, 128 MHz): −8.72 (s). UV−vis (CH_2Cl_2) λ nm (ϵ, M^{-1} cm^{-1}): 524 (84 000), 369 (111 000), 349 (100 700), 285 (113 500), 275 (105 500), 247 (140 400). IR (KBr): ν = 2962 (s), 2161 (m), 1642 (s), 1544 (s), 1180 (s), 977 (s), 845 (s). FAB$^+$ *m*/*z* (nature of peak, relative intensity): 917.2 ([M]$^+$, 100). Anal. Calcd for $C_{69}H_{49}BN_2$: C, 90.38; H, 5.39; N, 3.06. Found: C, 90.12; H, 5.12; N, 2.70.

4,4-Bis(pyrenyl-1-ethynyl-)-8-(4-iodophenyl)-1,3,5,7-tetramethyl-2,6-diethyl-4-bora-3a,4a-diaza-*s*-indacene (11). Prepared according to the general procedure with 1-ethynylpyrene (0.089 g, 0.39 mmol) in 10 mL of THF, 0.26 mL of *n*-butyllithium (1.55 M in *n*-hexane) (formation of a dark green anion), and 4,4-difluoro-8-(4-iodophenyl)-1,3,5,7-tetramethyl-4-bora-3a,4a-diaza-*s*-indacene **10** (0.1 g, 0.19 mmol) in 20 mL of THF. Complete consumption of the starting material was observed after 15 min. The chromatography was performed on alumina (CH_2Cl_2/cyclohexane, gradient from 10:90 to 30:70), and recrystallization gave 0.132 g of **11** (76% yield). ^{1}H NMR ($CDCl_3$ 400 MHz): δ = 8.78 (d, 2H, ^3J = 9.0 Hz), 8.17−7.97 (m, 16H), 7.88 (d, 2H, ^3J = 8.5 Hz), 7.22 (d, 2H, ^3J = 8.5 Hz), 3.16 (s, 6H), 2.47 (q, 4H, ^3J = 7.5 Hz), 1.44 (s, 6H), 1.11 (t, 6H, ^3J = 7.5 Hz). ^{13}C {^{1}H} NMR ($CDCl_3$, 75 MHz): 154.3, 138.8, 138.2, 136.3, 136.1, 133.4, 132.1, 131.3, 131.2, 130.7, 130.4, 129.6, 129.1, 127.8, 127.5, 127.3, 126.2, 126.0, 125.1, 124.6, 124.5, 124.4, 120.4, 94.5, 17.7, 15.1, 14.8, 12.5. ^{11}B {^{1}H }NMR ($CDCl_3$, 128 MHz): −8.94 (s). UV−vis (CH_2Cl_2) λ nm (ϵ, M^{-1} cm^{-1}): 523 (70 300), 370 (95 000), 350 (72 100), 285 (94 000), 274 (56 000), 247 (89 700). IR (KBr): ν = 3042 (m), 2961 (m), 2927 (s), 2169 (m), 1599 (m), 1543 (s), 1474 (s), 1434 (s), 1320 (s), 1180 (s), 978 (s), 845 (s), 747 (m). FAB$^+$ *m*/*z* (nature of peak, relative intensity): 919.1 ([M + H]$^+$, 100), 693.2 ([M−pyr−≡−]$^+$, 32). Anal. Calcd for $C_{59}H_{44}BIN_2$: C, 77.13; H, 4.83; N, 3.05. Found: C, 76.81; H, 4.51; N, 2.75.

4,4-Bis(pyrenyl-1-ethynyl-)8-(4-(ethyl hept-5-yn-oate)phenyl)-1,3,5,7-tetramethyl-2,6-diethyl-4-bora-3a,4a-diaza-*s*-indacene (12). To a degassed solution of **11** (0.1 g, 0.11 mmol) in THF/*i*Pr_2NH (10: 1.5 mL) was added ethyl hept-6-ynoate (0.25 g, 0.16 mmol). The solution was further degassed during 30 min, Pd(II)Cl_2(PPh_3)$_2$ (4 mg, 6% mol) and CuI (2 mg, 10% mol) were then added. The mixture was stirred at room temperature for 16 h, until the complete consumption of the starting material was observed. The solution was washed with water (50 mL), and extracted with CH_2Cl_2 (30 mL). The organic layers were dried over $MgSO_4$ and purified by chromatography on a column packed with alumina (cyclohexane/CH_2Cl_2, 80:30). Recrystallization in CH_2Cl_2/hexane gave **12** (0.09 g, 91% yield). ^{1}H NMR ($CDCl_3$, 300 MHz): 8.38 (d, 2H, ^3J = 9.2 Hz): 8.17−7.96 (m, 16H), 7.57 (d, 2H, ^3J = 8.1 Hz), 7.39 (d, 2H, ^3J = 8.1 Hz), 4.16 (q, 2H, ^3J = 7.2 Hz), 3.15 (s, 6H), 2.53−2.38

(m, 8H), 1.89−1.65 (m, 4H), 1.43 (s, 6H), 1.28 (t, 3H, ^3J = 7.2 Hz), 1.11 (t, 6H, ^3J = 7.3 Hz). $^{13}C\{^1H\}$NMR ($CDCl_3$, 75 MHz): 173.6, 154.2, 139.9, 136.6, 136.0, 133.3, 132.30, 132.27, 131.5, 130.5, 129.8, 129.4, 128.9, 127.9, 127.6, 127.5, 126.4, 126.1, 125.2, 124.73, 124.67, 124.5, 124.4, 120.7, 91.0, 80.8, 60.5, 34.0, 29.9, 28.3, 24.4, 19.4, 17.6, 15.0, 14.7, 14.4, 12.3. $^{11}B\{^1H\}$NMR ($CDCl_3$, 128 MHz): −8.97 (s). UV−vis (CH_2Cl_2) λ nm (ϵ, M^{-1} cm^{-1}): 523 (49 800), 370 (61 600), 350 (55 000), 285 (54 700), 274 (45 500), 250 (55 800). IR (KBr): ν = 2924 (m), 2165 (m), 1731 (s), 1543 (s), 1433 (s), 1180 (s), 978 (s), 847 (s). FAB^+ *m*/*z* (nature of peak, relative intensity): 945.2 ($[M]^+$, 100). Anal. Calcd for $C_{68}H_{57}BN_2O_2$: C, 86.43; H, 6.08; N, 2.96. Found: C, 86.19; H, 5.92; N, 2.60.

4,4-Bis(pyrenyl-1-ethynyl-)8-(4-(hept-5-yn-oic-acid)phenyl)-1,3,5,7-tetramethyl-2,6-diethyl-4-bora-3a,4a-diaza-*s*-indacene (13). A solution of ester **12** (0.09 g, 0.1 mmol) in ethanol/THF (10:10 mL) was heated for 12 h at 60 °C, in the presence of an excess of NaOH (1 M solution in H_2O, 9.7 mL, 1 mmol). After cooling, a diluted aqueous solution of HCl was added, until solution reached pH 5. The precipitate was filtered, dissolved in CH_2Cl_2 (50 mL), washed with two portions of water (100 mL), and dried over $MgSO_4$. Recrystallization in hot acetonitril gave pure **13** (0.079 g, 87% yield). ^1H NMR ($CDCl_3$, 300 MHz): 8.77 (d, 2H, ^3J = 9.0 Hz), 8.17−7.96 (m, 16H), 7.56 (d, 2H, ^3J = 8.3 Hz), 7.38 (d, 2H, ^3J = 8.3 Hz), 3.14 (s, 6H), 2.53−2.41 (m, 8H), 1.96−1.83 (m, 2H), 1.77−1.63 (m, 2H), 1.42 (s, 6H), 1.07 (t, 6H, ^3J = 7.6 Hz). ^{13}C $\{^1H\}$ NMR ($CDCl_3$, 75 MHz): 154.2, 139.9, 136.7, 136.0, 134.8, 133.3, 132.3, 132.2, 131.5, 131.3, 130.5, 129.8, 129.3, 128.8, 127.9, 127.6, 127.5, 126.4, 124.7, 124.6, 124.5, 124.4, 120.6, 33.3, 28.1, 19.4, 17.6, 15.0, 14.7, 12.3. ^{11}B $\{^1H\}$ NMR ($CDCl_3$, 128 MHz): −8.92 (s). UV−vis (CH_2Cl_2) λ nm (ϵ, M^{-1} cm^{-1}): 523 (58 100), 370 (75 000), 350 (66 400), 285 (67 200), 274 (56 300), 251 (67 600). IR (KBr): ν = 2962 (s), 2164 (m), 1633 (s), 1544 (s), 1180 (s), 977 (s), 846 (s). FAB^+ *m*/*z* (nature of peak, relative intensity): 917.2 ($[M + H]^+$, 25). Anal. Calcd for $C_{66}H_{53}BN_2O_2$: C, 86.45; H, 5.83; N, 3.06. Found: C, 86.23; H, 5.64; N, 2.79.

Succinimidyl Ester 14. To a solution of **13** (30 mg, 0.03 mmol) in 10 mL of CH_2Cl_2 were added (dimethylamino)pyridine (8.4 mg, 0.06 mmol), EDCI (12 mg, 0.06 mmol), and *N*-hydroxysuccinimide (7.2 mg, 0.06 mmol). The mixture was stirred at room temperature, for 1 h, until the complete consumption of the starting material was observed by TLC. The solution was then washed with water (10 mL), dried over $MgSO_4$, and purified by chromatography on a column packed with silica (CH_2Cl_2). Recrystallization in CH_2Cl_2/hexane gave pure **14** (18 mg, 54% yield). ^1H NMR ($CDCl_3$, 300 MHz): 8.78 (d, 2H, ^3J = 9.1 Hz), 8.17−7.96 (m, 18H), 7.56 (d, 2H, ^3J = 8.3 Hz), 7.39 (d, 2H, ^3J = 8.3 Hz), 3.14 (s, 6H), 2.9 (s, 4H), 2.73 (t, 2H, ^3J = 7.1 Hz), 2.53 (q, 4H, ^3J = 7.5 Hz), 2.04−1.94 (m, 2H), 1.82−1.73 (m, 2H), 1.43 (s, 6H), 1.10 (t, 6H, ^3J = 7.5 Hz). ^{13}C $\{^1H\}$ NMR ($CDCl_3$, 75 MHz): 169.2, 168.2, 154.2, 136.7, 136.0, 133.3, 132.35, 132.34, 132.28, 131.8, 131.5, 130.5, 129.8, 129.4, 128.9, 127.9, 127.6, 127.5, 126.4, 126.1, 125.2, 124.8, 124.7, 124.5, 124.3, 120.7, 90.5, 30.7, 27.8; 25.8, 24.0, 19.2, 17.6, 15.0, 14.7, 12.3. ^{11}B $\{^1H\}$ NMR ($CDCl_3$, 128 MHz): −8.98 (s). UV−vis (CH_2Cl_2) λ nm (ϵ, M^{-1} cm^{-1}): 523 (55 000), 370 (70 000), 350 (56 000), 285 (81 000), 274 (57 000), 248 (88 000). IR (KBr): ν = 3435 (m), 2960 (s), 2927 (s), 2230 (m), 2169 (m), 1741 (s), 1543 (s), 1431 (s), 1180 (s), 978 (s), 848 (s). Anal. Calcd for $C_{70}H_{56}BN_3O_4$: C, 82.91; H, 5.57; N, 4.14. Found: C, 82.68; H, 5.32; N, 3.79.

Amide 15. A solution of **14** (10 mg, 0.01 mmol) in 10 mL of *n*-propylamine was stirred for 1 h at room temperature. The amine was then evaporated, and the solid was extracted with two portions of CH_2Cl_2 (20 mL), then washed with two portions of water (20 mL). The crude product was purified by column chromatography on silica gel (CH_2Cl_2/MeOH, gradient from 100:0 to 95:5), yielding pure **15** (7 mg, 74%). ^1H NMR ($CDCl_3$, 300 MHz): 8.78 (d, 2H, ^3J = 9.0 Hz), 8.17−7.96 (m, 16H), 7.56 (d, 2H, ^3J = 8.3 Hz), 7.38 (d, 2H, ^3J = 8.3 Hz), 3.27 (m, 2H), 3.14 (s, 6H), 2.52−2.42 (m, 6H), 2.25 (t, 2H, ^3J = 7.2 Hz), 1.98−1.85 (m, 2H), 1.74−1.66 (m, 2H), 1.53 (q, 2H, ^3J = 7.2 Hz), 1.42 (s, 6H), 1.10 (t, 6H, ^3J = 7.4 Hz), 0.93 (t, 3H, ^3J = 7.4 Hz). ^{13}C $\{^1H\}$ NMR ($CDCl_3$, 75 MHz): 172.7, 154.2, 139.9, 136.6, 136.0, 133.3, 132.29, 132.27, 131.5, 131.3, 130.5, 129.8, 129.3, 128.8, 127.9, 127.6, 127.5, 126.4, 126.1, 125.3, 124.7, 124.6, 124.5, 124.4, 120.6, 91.1, 41.4, 36.5, 28.4, 25.2, 23.2, 19.4, 17.6, 15.0, 14.7, 12.3, 11.5. ^{11}B $\{^1H\}$ NMR ($CDCl_3$, 128 MHz): −8.98 (s). UV−vis (CH_2Cl_2) λ nm (ϵ, M^{-1} cm^{-1}): 523 (60 700), 370 (88 000), 350 (70 000), 285 (91 000), 274 (57 000), 248 (103 000). IR (KBr): ν = 2962 (s), 2317 (m), 2172 (s), 1711 (m), 1648 (s), 1543 (s), 1180 (s), 847 (s). FAB^+ *m*/*z* (nature of peak, relative intensity): 958.2 ($[M]^+$, 100). Anal. Calcd for $C_{69}H_{60}BN_3O$: C, 86.50 H, 6.31; N, 4.39. Found: C, 86.32; H, 6.13; N, 4.03.

Acknowledgment. The authors thank CNRS and IST/ILO Contract 2001-33057 for funding. G.U. thanks ANR for supporting "Borsupstokes" Project JC05-42228. We are also indebted to Professor Jack Harrowfield (ISIS Strasbourg) for the careful reading of and commenting on this manuscript prior to publication. The cover background shows an NPS photo of Undine Falls, Yellowstone National Park, by Jim Peaco, March 2002.

Supporting Information Available: General experimental procedure, reagents, materials**,** experimental details for compounds **2**, **4**, **6**, **7**, **8**, **9b**,**c**; CCDC numbers for X-ray structures of compounds **2** and **4**. This material is available free of charge via the Internet at http://pubs.acs.org.

JO060984W